

Multiplicity Fluctuations in Nucleus-Nucleus Collisions: Dependence on Energy and Atomic Number

V.P. Konchakovski,^{1,2} B. Lungwitz,³ M.I. Gorenstein,^{2,4} and E.L. Bratkovskaya⁴

¹*Helmholtz Research School, University of Frankfurt, Frankfurt, Germany*

²*Bogolyubov Institute for Theoretical Physics, Kiev, Ukraine*

³*Institut für Kernphysik, University of Frankfurt, Frankfurt, Germany*

⁴*Frankfurt Institute for Advanced Studies, Frankfurt, Germany*

Abstract

Event-by-event multiplicity fluctuations in central C+C, S+S, In+In, and Pb+Pb as well as p+p collisions at bombarding energies from 10 to 160 AGeV are studied within the HSD and UrQMD microscopic transport approaches. Our investigation is directly related to the future experimental program of the NA61 Collaboration at the SPS for a search of the QCD critical point. The dependence on energy and atomic mass number of the scaled variances for negative, positive, and all charged hadrons is presented and compared to the results of the model of independent sources. Furthermore, the nucleus-nucleus results from the transport calculations are compared to inelastic proton-proton collisions for reference. We find a dominant role of the participant number fluctuations in nucleus-nucleus reactions at finite impact parameter b . In order to reduce the influence of the participant numbers fluctuations on the charged particle multiplicity fluctuations only the most central events have to be selected. Accordingly, the samples of the 1% most central nucleus-nucleus collisions with the largest numbers of the projectile participants are studied. The results are compared with those for collisions at zero impact parameter. A strong influence of the centrality selection criteria on the multiplicity fluctuations is pointed out. Our findings are essential for an optimal choice of colliding nuclei and bombarding energies for the experimental search of the QCD critical point.

PACS numbers: 24.10.Lx, 24.60.Ky, 25.75.-q

Keywords:

I. INTRODUCTION

The event-by-event fluctuations in high energy nucleus-nucleus (A+A) collisions (see e.g., the reviews [1, 2, 3]) are expected to be closely related to the transitions between different phases of QCD matter. By measuring the fluctuations one should observe anomalies from the onset of deconfinement [4] and dynamical instabilities when the expanding system goes through the 1-st order transition line between the quark-gluon plasma (QGP) and the hadron gas [5]. Furthermore, the QCD critical point may be signaled by a characteristic pattern in enhanced fluctuations. A+A collisions in the SPS energy region are expected to be a suitable tool for a search of critical point signatures [6]. Only recently first measurements of particle multiplicity fluctuations [7] and transverse momentum fluctuations [8] in A+A collisions have been performed. A theoretical analysis of multiplicity fluctuations for the hadron-resonance gas - in different statistical ensembles - has been performed in Ref. [9]. Independently, the multiplicity fluctuations in A+A collisions has been studied within a microscopic transport approach [10, 11]. We recall that fluctuations traditionally are quantified by the ratio of the variance of the multiplicity distribution to its mean value, the scaled variance. Previous works on this subject have to be quoted. The calculations of the statistical models [13] and transport approaches HSD [14] and UrQMD v. 1.3 [15] have been compared with the corresponding preliminary results [16] of the NA49 Collaboration in central Pb+Pb collisions at SPS energies. At RHIC energies a HSD analysis of the preliminary data [17] of the PHENIX Collaboration in Au+Au collisions at $\sqrt{s_{NN}} = 200$ GeV has been presented in Ref. [18].

An ambitious experimental program for the search of the QCD critical point has been started by the NA61 Collaboration at the SPS [19]. The program includes a variation in the atomic mass number A of the colliding nuclei as well as an energy scan. This allows to scan the phase diagram in the plane of temperature T and baryon chemical potential μ_B near the critical point as argued in Ref. [19]. One expects to ‘locate’ the position of the critical point by studying its ‘fluctuation signals’. High statistics multiplicity fluctuation data will be taken for p+p, C+C, S+S, In+In, and Pb+Pb collisions at bombarding energies of $E_{lab}=10, 20, 30, 40, 80,$ and 158 AGeV.

The aim of the present paper is to study the energy and system size dependence of event-by-event multiplicity fluctuations within the microscopic transport approaches Hadron-String-Dynamics (HSD, v. 2.5) [20] and Ultra-Relativistic-Quantum-Molecular-Dynamics (UrQMD,

v 1.3) [21]. These models provide a rather reliable description (see, e.g., Refs. [21, 22]) for the inclusive spectra of charged hadrons in A+A collisions from SIS to RHIC energies. In our study we will consider C+C, S+S, In+In, and Pb+Pb collisions at the bombarding energies of 10, 20, 30, 40, 80, 158 AGeV. For a comparison and reference we also present the results of multiplicity fluctuations in p+p collisions at the same energies. Our study thus is in full correspondence to the experimental program of the NA61 Collaboration [19]. In order to estimate systematical errors from the theoretical side we employ the two independent transport models (HSD and UrQMD) as in Ref. [22].

The QCD critical point is expected to be experimentally seen as a non-monotonic dependence of the multiplicity fluctuations, i.e. a specific combination of atomic mass number A and bombarding energy E_{lab} could move the chemical freeze-out of the system close to the critical point and show a ‘spike’ in the multiplicity fluctuations. Since HSD and UrQMD do not include explicitly a phase transition from a hadronic to a partonic phase, we can not make a clear suggestion for the location of the critical point - it is beyond the scope of our hadron-string models. However, our study might be helpful in the interpretation of the upcoming experimental data since it will allow to subtract simple dynamical and geometrical effects from the expected QGP signal. The deviations of the future experimental data from the HSD and UrQMD predictions may be considered as an indication for the critical point signals.

Theoretical estimates give about 10% increase of the multiplicity fluctuations due to the critical point [6]. It is large enough to be observed experimentally within the statistics of NA61 [19]. To achieve this goal, it is necessary to have a control on other possible sources of fluctuations. One of such sources is the fluctuation of the number of nucleon participants. It has been found in Ref. [10] that these fluctuations give a dominant contribution to hadron multiplicity fluctuations in A+A collisions. On the other hand one can suppress the participant number fluctuations by selecting most central A+A collisions (see Ref. [10, 23] for details). That’s why the NA61 Collaboration plans to measure central collisions of light and intermediate ions instead of peripheral Pb+Pb collisions. It is important to stress, that the conditions for the centrality selection in the measurement of fluctuations are much more stringent than those for mean multiplicity measurements. This issue will be discussed in detail in our paper.

Our paper is organized as follows. In Section II the HSD and UrQMD models are compared with the data for the charged hadron multiplicity, mean values and fluctuations in p+p collisions

in the SPS energy range 10 – 158 AGeV. In Section III the participant number fluctuations in fixed target experiments are discussed and estimated within HSD and UrQMD. In Section IV we present the HSD and UrQMD results for the charged hadron multiplicity fluctuations in $A + A$ collisions with zero impact parameter, $b = 0$. The participant number fluctuations in $A + A$ collisions at $b = 0$ are considered in Section V. In addition, the transport model results for the charged hadron multiplicity fluctuations are compared within the model of independent sources. In Section VI the centrality selection - by fixing the number of projectile participants - is considered and compared to the case of $b = 0$. Section VI presents also the HSD and UrQMD results for the charged hadron multiplicity fluctuations in $A + A$ collisions for the 1% most central collisions corresponding to the largest number of projectile participants. A summary and conclusion will close the paper in Section VII.

II. MULTIPLICITY FLUCTUATIONS IN PROTON-PROTON COLLISIONS

For a quantitative measure of the particle number fluctuations it is convenient to use the scaled variances,

$$\omega_i \equiv \frac{\langle N_i^2 \rangle - \langle N_i \rangle^2}{\langle N_i \rangle}, \quad (1)$$

where $\langle \dots \rangle$ denotes event-by-event averaging and the index i means “-”, “+”, and “ch”, i.e. negative, positive, and all charged final state hadrons.

The energy dependence of the measured charged multiplicity and fluctuations for p+p collisions can be parametrized by the functions [1]:

$$\langle N_{ch} \rangle \cong -4.2 + 4.69 \left(\frac{\sqrt{s_{NN}}}{\text{GeV}} \right)^{0.31}, \quad \omega_{ch} \cong 0.35 \frac{(\langle N_{ch} \rangle - 1)^2}{\langle N_{ch} \rangle}, \quad (2)$$

where $\sqrt{s_{NN}}$ is the center-of-mass energy.

Figure 1 shows the HSD and UrQMD results for inelastic p+p collisions in comparison to the experimental data taken from Ref. [1]. As seen from Fig. 1 both models give a good reproduction of the p+p data for $\langle N_{ch} \rangle$, but slightly (over) underestimate ω_{ch} at high collision energies. The differences between the HSD and UrQMD model results for ω_{ch} can be attributed to different realizations of the string fragmentation model, in particular, differences in the fragmentation functions and the fragmentation scheme, i.e. fragmentation via heavy baryonic

and mesonic resonances in UrQMD and direct light hadron production by string fragmentation in HSD.

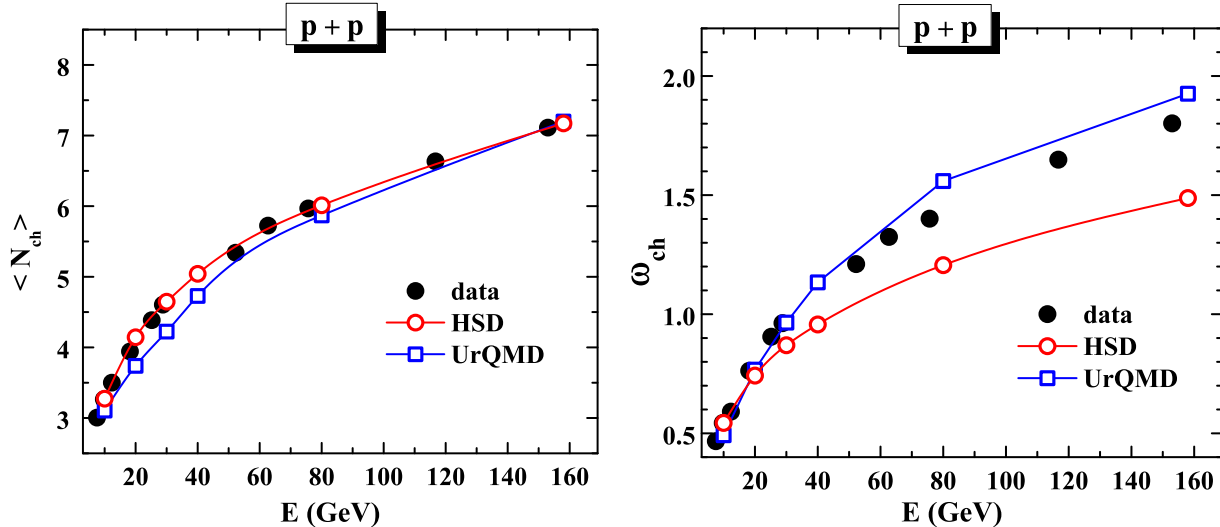


FIG. 1: (Color online) The average multiplicity (*left*) and scaled variance (*right*) of charged hadrons in p+p inelastic collisions. The open circles and squares (connected by solid lines) show the results of HSD and UrQMD, respectively, whereas the full circles present the experimental data from Ref. [1].

For negative and positive charged hadrons the average multiplicities and scaled variances in p+p collisions can be presented in terms of the corresponding quantities for all charged particles,

$$\langle N_{\pm} \rangle = \frac{1}{2} (\langle N_{ch} \rangle \pm 2) , \quad \omega_{\pm} = \frac{1}{2} \omega_{ch} \frac{\langle N_{ch} \rangle}{\langle N_{ch} \rangle \pm 2} . \quad (3)$$

III. PARTICIPANT NUMBER FLUCTUATIONS

In each $A + A$ collision only a fraction of all $2A$ nucleons, i.e. the participants, interact. Participants from the projectile and target nuclei are denoted as N_P^{proj} and N_P^{targ} , respectively. The nucleons, which do not interact, are denoted as projectile and target spectators, $N_S^{proj} = A - N_P^{proj}$ and $N_S^{targ} = A - N_P^{targ}$. The spectators are selected according to the criteria $|y_{beam(target)}| \leq 0.32$ and excluded from the multiplicity fluctuation analysis. We recall that fluctuations in high energy $A + A$ collisions are dominated by a geometrical variation of the impact parameter b . However, even for fixed impact parameter b the number of participants, $N_P \equiv N_P^{proj} + N_P^{targ}$, fluctuates from event to event. This is due to fluctuations in the initial

states of the colliding nuclei and the probabilistic character of the interaction process. These fluctuations of N_P form usually a large and uninteresting background.

To minimize the event-by-event fluctuations of the number of nucleon participants in measuring the multiplicity fluctuations the NA49 Collaboration has been trying to fix N_P^{proj} in Pb+Pb collisions. Samples of collisions with a fixed number of projectile spectators, $N_S^{proj} = const$ (and thus a fixed number of projectile participants, N_P^{proj}), have been selected. This selection is possible in fixed target experiments at the SPS, where N_S^{proj} is measured by a Zero Degree Veto Calorimeter covering the projectile fragmentation domain. A similar centrality selection is expected to be implemented in the future NA61 experiment. However, even in samples with $N_P^{proj} = const$ the number of target participants will fluctuate considerably. Hence, an asymmetry between projectile and target participants is introduced, i.e. N_P^{proj} is constant by constraint, whereas N_P^{targ} fluctuates independently (the consequences of this asymmetry have been discussed in Ref. [23]).

In each sample with $N_P^{proj} = const$ the number of target participants fluctuates around its mean value with the scaled variance ω_P^{targ} . The mean value equals to $\langle N_P^{targ} \rangle \cong N_P^{proj}$, if N_P^{proj} is not too close to its limiting values, $N_P^{proj} = 1$ and $N_P^{proj} = A$. The scaled variance of target participants ω_P^{targ} as a function of fixed number of projectile participants N_P^{proj} has been obtained from HSD and UrQMD in Ref. [10] for Pb+Pb collisions at 158 AGeV.

Fig. 2 (*left*) presents the HSD scaled variances ω_P^{targ} for C+C, S+S, In+In, and Pb+Pb collisions at 158 AGeV as a function of N_P^{proj} . The fluctuations of N_P^{targ} are quite strong for peripheral reactions (small N_P^{proj}) and negligible for the most central collisions (large N_P^{proj}). A vanishing of $\omega_P^{targ} \cong 0$ at $N_P^{proj} \cong A$ does not, however, show up in C+C collisions. Even for $N_P^{proj} = A = 12$ in C+C collisions the number of participants from the target still fluctuates and the scaled variance amounts to $\omega_P^{targ} \cong 0.25$. Fig. 2 (*right*) shows ω_P^{targ} for light nuclei, S+S, Ne+Ne, O+O, and C+C. Even for the maximal values of $N_P^{proj} = A$ the fluctuations ω_P^{targ} do not vanish and increase with decreasing atomic mass number A .

The temperature T and baryon chemical potential μ_B at the hadron chemical freeze-out demonstrate the dependence on both the collision energy and system size [12]. Thus, changing the number of participating nucleons one may scan the $T - \mu_B$ plane. Some combination of N_P and E_{lab} might move the chemical freeze-out point close the QCD critical point. One could then expect an increase of multiplicity fluctuations in comparison to their ‘background values’.

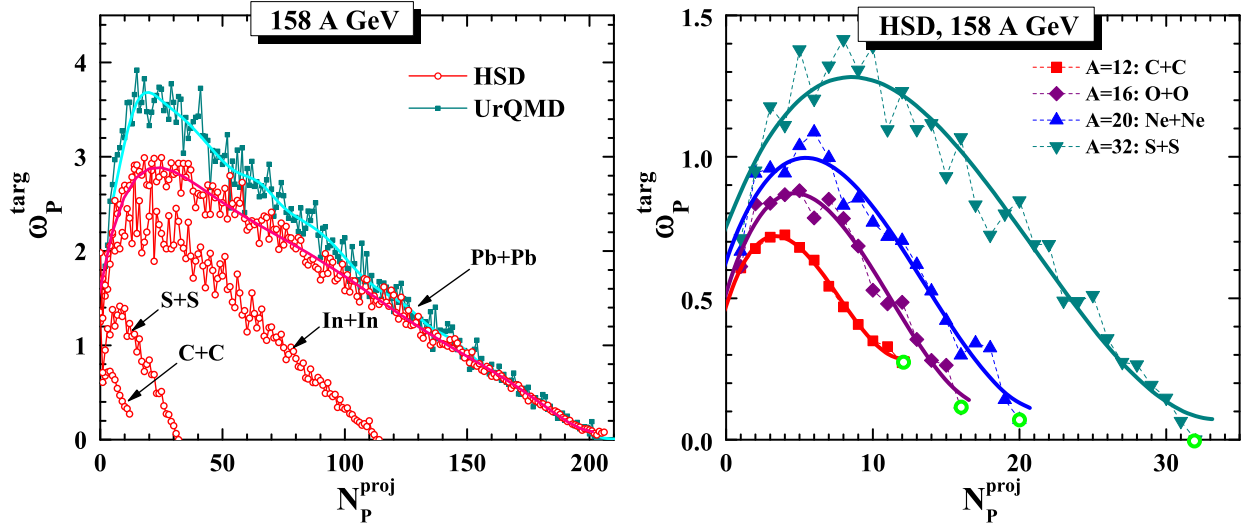


FIG. 2: (Color online) *Left:* The scaled variance ω_P^{targ} for the fluctuations of the number of target participants, N_P^{targ} . The HSD simulations of ω_P^{targ} as a function of N_P^{proj} are shown for different colliding nuclei, In+In, S+S, and C+C at $E_{lab}=158$ AGeV. The HSD and UrQMD results for Pb+Pb collisions are taken from Ref. [10]. *Right:* The scaled variance ω_P^{targ} for light nuclei, S+S, Ne+Ne, O+O, and C+C at $E_{lab}=158$ AGeV as a function of N_P^{proj} . Fluctuations of target participants for $N_P^{proj}=A$ - shown by the open symbols - are different from zero and increase with decreasing atomic mass number A .

Why does one need central collisions of light and intermediate ions instead of studying peripheral Pb+Pb collisions for a search of the critical point? Fig. 2 explains this issue. At fixed N_P^{proj} the average total number of participants, $N_P \equiv N_P^{proj} + N_P^{targ}$, is equal to $\langle N_P \rangle \cong 2N_P^{proj}$, and, thus, it fluctuates as $\omega_P = 0.5\omega_P^{targ}$. Then, for example, the value of $N_P^{proj} \cong 30$ corresponds to almost zero participant number fluctuations, $\omega_P \cong 0$, in S+S collisions while ω_P becomes large and is close to 1 and 1.5 for In+In and Pb+Pb, respectively. Even if N_P^{proj} is fixed exactly, the sample of the peripheral collision events in the heavy-ion case contains large fluctuations of the participant number: this would ‘mask’ the critical point signals. As also seen in Fig. 2 (*right*), the picture becomes actually more complicated if the atomic mass number A is too small. In this case, the number of participants from a target starts to fluctuate significantly even for the largest and fixed value of $N_P^{proj}=A$.

IV. MULTIPLICITY FLUCTUATIONS AT ZERO IMPACT PARAMETER

A. Centrality Selection in A+A Collisions by Impact Parameter

The importance of a selection of the most central collisions for studies of hadron multiplicity fluctuations has been stressed in our previous papers [10, 11, 14, 18]. Due to its convenience in theoretical studies (e.g., in hydrodynamical models) one commonly uses the condition on impact parameter b , for the selection of the ‘most central’ collisions in model calculations. However, the number of participant even at $b = 0$ is not strictly fixed, and fluctuates according to some distributions (cf. Fig. 14 (*right.*) from Ref. [11]). It should be stressed again that the conditions $b < b_{max}$ can not be fixed experimentally since the impact parameter itself can not be measured in a straightforward way. Actually, in experiments one accounts for the 1%, 2% etc. most central events selected by the measurement of spectators in the Veto calorimeter, which corresponds to the event class with the largest N_P^{proj} . As we will demonstrate below the multiplicity fluctuations are very sensitive to the centrality selection criteria. In particular, the transport model results for $b = 0$ and for 1% events with the largest N_P^{proj} are rather different (see below).

Let’s start with the $b = 0$ centrality selection criterium. We recall that the charged multiplicity fluctuations are closely related to the fluctuations of the number of participants [10, 14]. Therefore, it is useful to estimate the average number of participants, $\langle N_P \rangle$, and the scaled variances of its fluctuations, ω_P , in $A + A$ collision events which satisfy the $b = 0$ condition. The left panel in Fig. 3 shows the ratio, $\langle N_P \rangle / 2A$, in $A + A$ collisions with $b = 0$ for different nuclei at collision energies $E_{lab} = 10$ and 158 AGeV. Both transport models (HSD and UrQMD) show a monotonous increase of $\langle N_P \rangle / 2A$ with collision energy for all nuclei in the energy range $10 \div 158$ AGeV (Fig. 3, *left*). Correspondingly, the fluctuations of the number of participants ω_P for all nuclei become smaller with increasing collision energy (Fig. 3, *right*). As seen from Fig. 3 (*left*) about 90% of nucleons are participants for Pb+Pb collisions with $b = 0$. This number becomes essentially smaller, about 60-70%, for C+C collisions. One can therefore expect that participant number fluctuations at $b = 0$ are small for heavy nuclei but strongly increase for light systems. This is demonstrated in Fig. 3 (*right*): ω_P is about $0.1 \div 0.2$ in Pb+Pb and In+In but becomes much larger, $0.5 \div 0.7$, in C+C collisions.

One can conclude that the condition $b = 0$ corresponds to ‘most central’ $A + A$ collisions

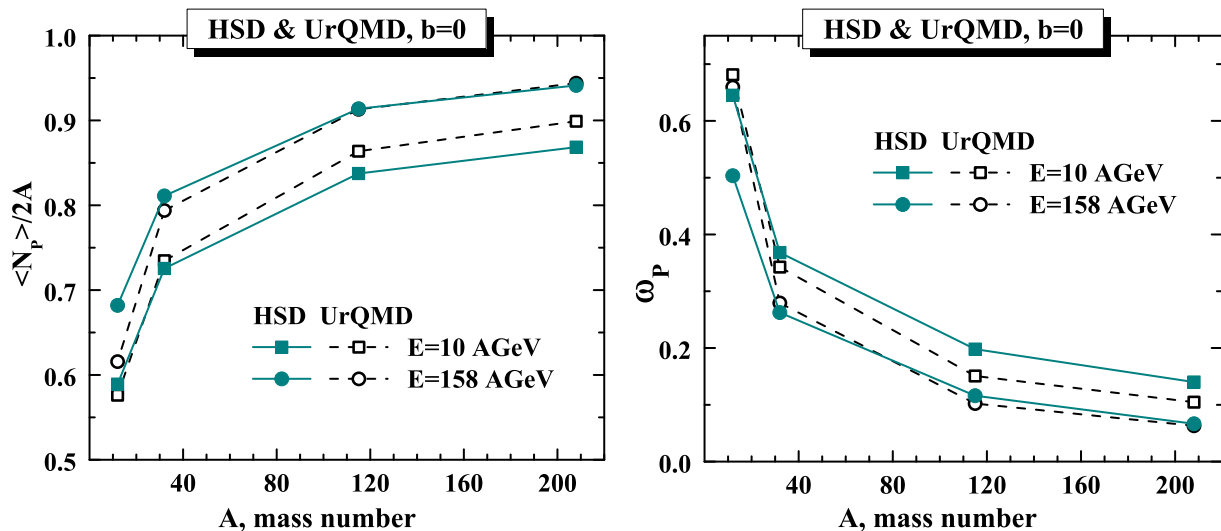


FIG. 3: (Color online) *Left*: Mean $\langle N_P \rangle$, divided by the maximum number of participants $2A$ in events with $b = 0$ for different nuclei at collision energies $E_{lab}=10$ and 158 AGeV. *Right*: The scaled variance ω_P in events with $b = 0$ for different nuclei at collision energies $E_{lab}=10$ and 158 AGeV.

only for nuclei with large atomic mass number (In and Pb). In this case the average number of participants is close to its maximum value and its fluctuations are rather small. However, in the studies of event-by-event multiplicity fluctuations in the collisions of light nuclei (C and S) the criterium $b = 0$ is far from selecting the ‘most central’ $A + A$ collisions.

B. HSD and UrQMD Results for the Multiplicity Fluctuations for $b=0$

Results of HSD and UrQMD transport model calculations for the scaled variance of negative, ω_- , positive, ω_+ , and all charged, ω_{ch} , hadrons are shown in Figs. 4 and 5 at different collision energies, $E_{lab} = 10, 20, 30, 40, 80, 158$ AGeV, and for different colliding nuclei, C+C, S+S, In+In, Pb+Pb. The transport model results correspond to collision events for zero impact parameter, $b = 0$. To make the picture more complete, the transport model results for inelastic p+p collisions are shown too, for reference. Note that in our presentation - throughout the paper - the proton spectators are not accounted for in the calculation of N_+ and N_{ch} . Thus, proton spectators do not contribute to ω_+ and ω_{ch} .

One sees a monotonic dependence of the multiplicity fluctuations on both E_{lab} and A : the scaled variances ω_- , ω_+ , and ω_{ch} increase with E_{lab} and decrease with A . The results for

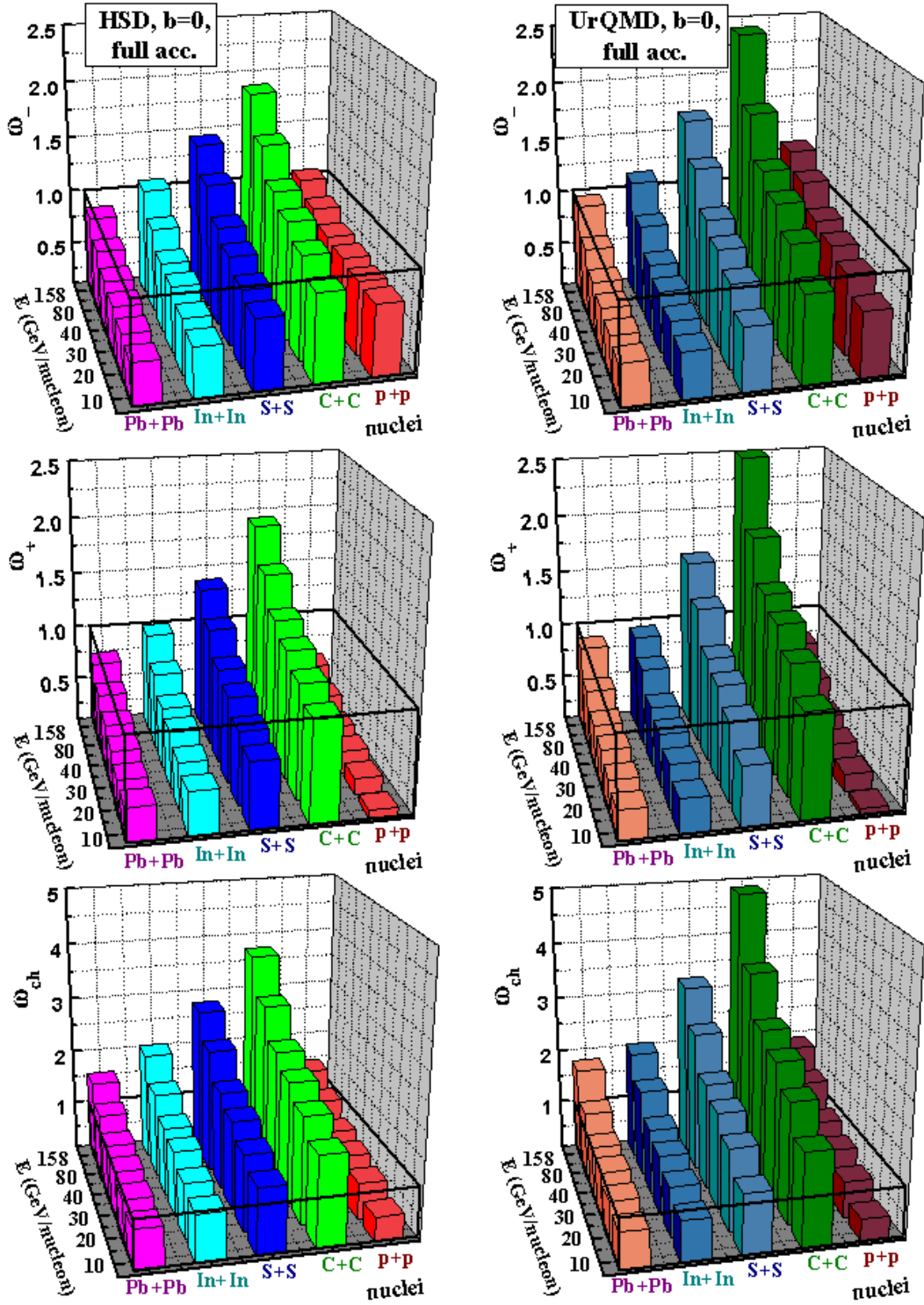


FIG. 4: (Color online) The results of HSD (*left*) and UrQMD (*right*) simulations for ω_- (top panel), ω_+ (middle panel), and ω_{ch} (lower panel) in p+p and central C+C, S+S, In+In, Pb+Pb collisions at $E_{lab} = 10, 20, 30, 40, 80, 158$ AGeV. The condition $b = 0$ is used here as a criterion for centrality selection. There are no cuts in acceptance.

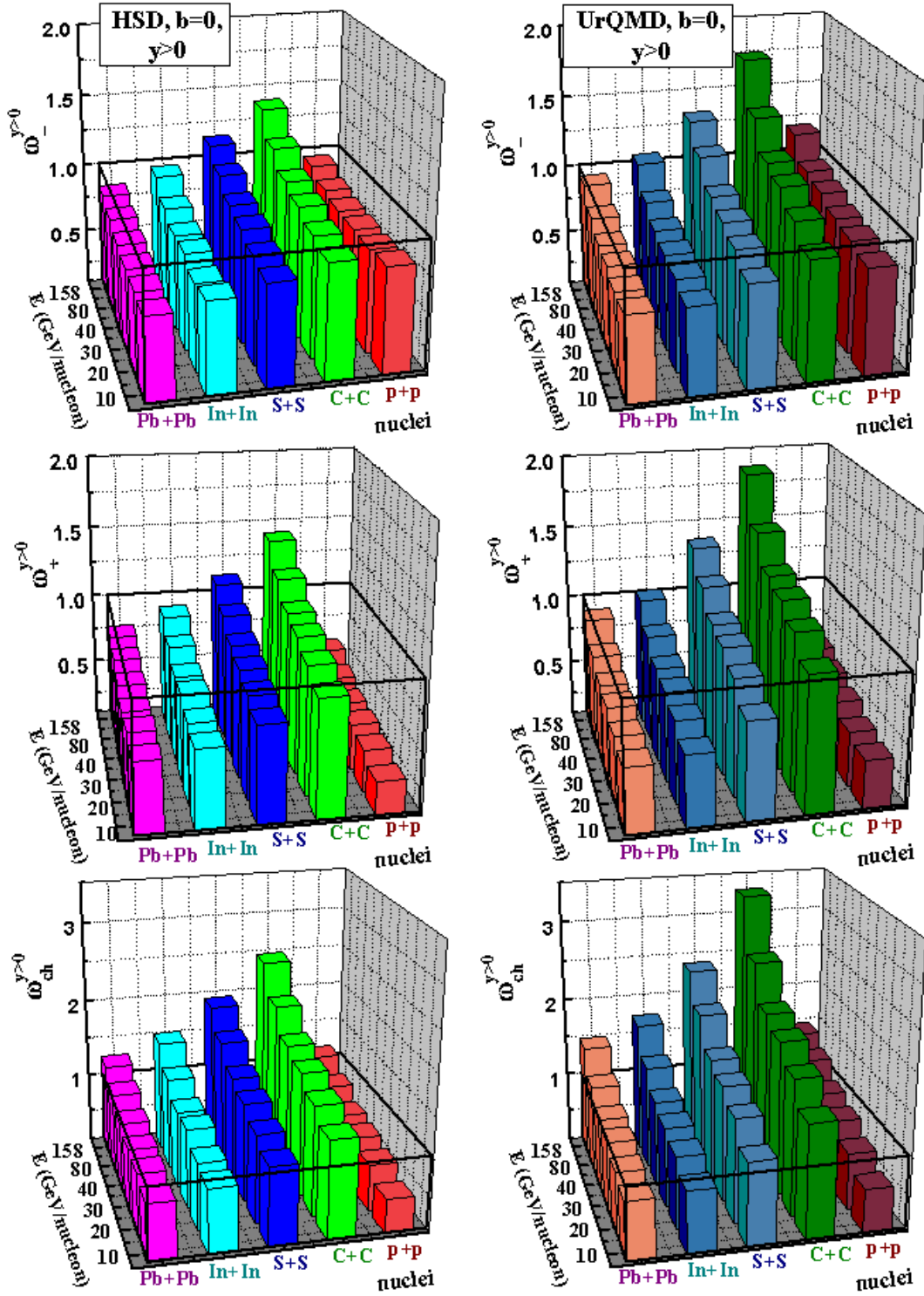


FIG. 5: (Color online) The same as in Fig. 4, but only hadrons with positive c.m. rapidities, $y > 0$ (projectile hemisphere), are accepted.

p+p collisions are different from those for light ions. We note that within HSD and UrQMD a detailed comparison of the multiplicity fluctuations in nucleon-nucleon inelastic collisions and $b = 0$ heavy-ion collisions (Pb+Pb and Au+Au), including the energy dependence up to $\sqrt{s_{NN}} = 200$ GeV, has been presented in Refs. [14, 15].

Fig. 4 corresponds to the full 4π acceptance, i.e. all particles are accepted without any cuts in phase space. In actual experiments the detectors accept charged hadrons in limited regions of momentum space. Fig. 5 shows the HSD and UrQMD results for multiplicity fluctuations in the projectile hemisphere (i.e. positive rapidities, $y > 0$ in the c.m. frame). This corresponds to the maximal possible acceptance, up to 50% of all charged particles, by the optimized detectors of the NA61 Collaboration [19]. One observes from Fig. 5 that the energy and system size dependencies of the multiplicity fluctuations in the projectile hemisphere ($y > 0$) become less pronounced than in full 4π acceptance. Note also that the centrality selection criterium $b = 0$ keeps the symmetry between the projectile and target hemispheres. Thus, the results for a $y < 0$ acceptance are identical to those for $y > 0$ presented in Fig. 5.

C. Comparison to the Independent Source Model

The multiplicity fluctuations in elementary nucleon-nucleon collisions and fluctuations of the number of nucleon participants are presented in the right panels of Figs. 1 and 3, respectively. Their combination explains the main features of hadron multiplicity fluctuations in $A + A$ collisions shown in Figs. 4 and 5, in particular, the dependence on collision energy and atomic mass number. They also are responsible for the larger values of ω_i in the UrQMD simulations in comparison to those from HSD. To illustrate this let us consider the model of independent sources (ISM).

The multiplicity fluctuations in $A + A$ collisions can be then written according to the ISM as (see e.g., Refs. [1, 10, 14, 18, 23]),

$$\omega_i = \omega_i^* + n_i \omega_P , \quad (4)$$

where ω_i^* denotes the fluctuations of the hadron multiplicity from one source and the term $n_i \omega_P$ gives additional fluctuations due to the fluctuations of the number of sources. One usually assumes that the number of sources is proportional to the number of nucleon participants. The value of n_i in Eq. (4) then is the average number of i 'th particles per participant, $n_i =$

$\langle N_i \rangle / \langle N_P \rangle$, and ω_P equals the scaled variance for the number of nucleon participants. Nucleon-nucleon collisions, which are the weighted combinations of p+p, p+n, and n+n reactions, define the fluctuations ω_i^* from a single source (see details in Refs. [10, 14]).

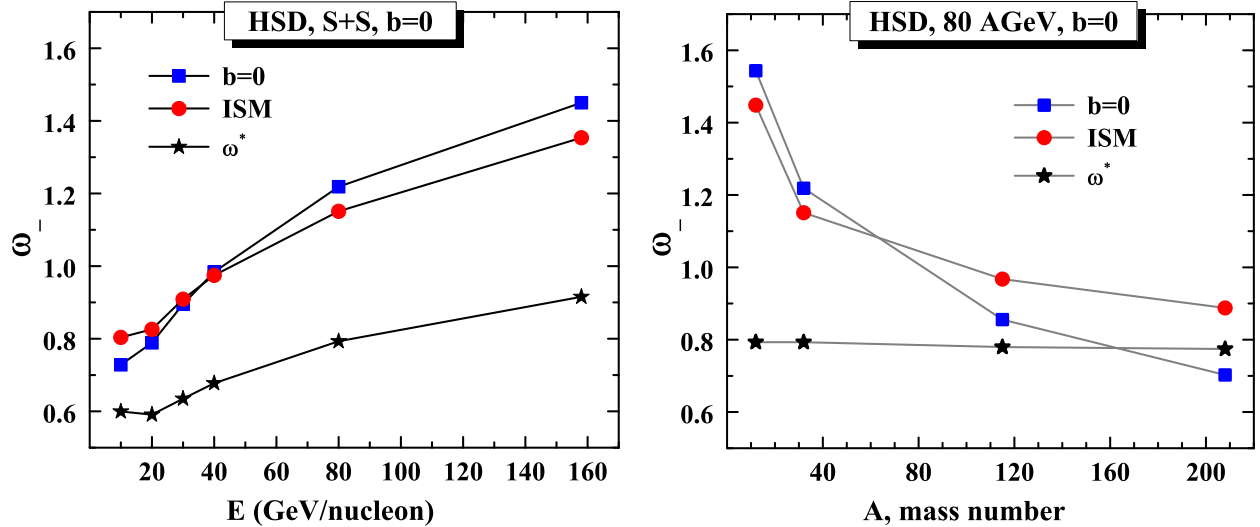


FIG. 6: (Color online) The *left* panel illustrates the energy dependence of ω_- in S+S collisions at $b = 0$ in the full 4π acceptance, the *right* panel – the ω_- dependence on atomic mass number at $E_{lab}=80$ AGeV. The HSD results are shown by the squares while the circles correspond to Eq. (4) of the model of independent sources. The stars show the first term, ω_-^* , in the *right*. of Eq. (4) – scaled variance for negative hadrons in nucleon-nucleon collisions, where the values of ω_-^* , n_i , and ω_P are calculated within HSD.

In Fig. 6 the HSD results for ω_i in $A + A$ collisions at $b = 0$ are compared to the ISM – Eq. (4). One concludes that the transport model results for the multiplicity fluctuations are in qualitative agreement with Eq. (4) of the independent source model. Both n_i and ω_i^* increase strongly with collision energy as seen from Fig. 1. This explains, due to Eq. (4), the monotonous increase with energy of the scaled variances ω_i in $A + A$ collisions at $b = 0$ seen in Figs. 4 and 5. Note that ω_P at $b = 0$ decreases with collision energy as shown in Fig. 3, *right*. This, however, does not compensate a strong increase of both n_i and ω_i^* . The atomic mass number dependence of the scaled variances ω_i in $A + A$ collisions with $b = 0$ follows from the A -dependence of ω_P . Fig. 3 (*right*) demonstrates a strong increase of ω_P for light nuclei. This, due to Eq. (4), is transformed to the corresponding behavior of ω_i seen in Figs. 4 and 5.

V. MULTIPLICITY FLUCTUATIONS IN 1% MOST CENTRAL COLLISIONS

We consider now the centrality selection procedure by fixing the number of projectile participants N_P^{proj} . This corresponds to the real situation of $A + A$ collisions in fixed target experiments. As a first step we simulate in HSD and UrQMD the minimal bias events - which correspond to an all impact parameter sample - and calculate the event distribution over the number of participants N_{part} . Then, we select 1% most central collisions which correspond to the largest values of N_P^{proj} . In such a sample of $A+A$ collisions events with largest N_P^{proj} from different impact parameters can contribute. After that we calculate the values of ω_P in these samples. Note that even for a fixed number of N_P^{proj} the number of target participants N_P^{targ} fluctuates. Thus, the total number of participants, $N_P = N_P^{targ} + N_P^{proj}$, fluctuates too. In our 1% sample, both N_P^{targ} and N_P^{proj} fluctuate. Besides, there are correlations between N_P^{targ} and N_P^{proj} .

Fig. 7 shows the ratio $\langle N_P \rangle / 2A$ and the scaled variance, ω_P , for 1% most central collisions selected by the largest values of N_P^{proj} . These results are compared with those for the $b = 0$ centrality selection. For heavy nuclei, like In and Pb, one finds no essential differences between these two criteria of centrality selection. However, the 1% centrality trigger defined by the largest values of N_P^{proj} looks much more rigid for light ions (S and C). In this case, the ratio $\langle N_P \rangle / 2A$ is larger, and ω_P is essentially smaller than for the criterion $b = 0$. As a result, the 1% centrality trigger by the largest values of N_P^{proj} leads to a rather weak A -dependence of ω_P .

Some comments are appropriate at this point. Let us define the centrality $c(N)$ as a percentage of events with a multiplicity larger than N (this can be the number of produced hadrons, number of participants, etc.). It was argued in Ref. [24] that a selection of $c(N)$ of most central $A + A$ collisions is equivalent to restricting the impact parameter, $b < b(N)$, with,

$$b(N) = \sqrt{\frac{\sigma_{inel}}{\pi} c(N)}, \quad (5)$$

where σ_{inel} is the total inelastic $A+A$ cross section. Thus, the centrality criterion by the multiplicity N is equivalent to the geometrical criterion by the impact parameter b . Moreover, the result (5) does not depend on the specific observable N used to define the c -percentage of most central $A+A$ collisions. Eq. (5) should remain the same for any observable N which is a monotonic function of b . Therefore, the relation (5) reduces any centrality selection to the geometrical one. This result was obtained in Ref. [24] by neglecting the fluctuations of

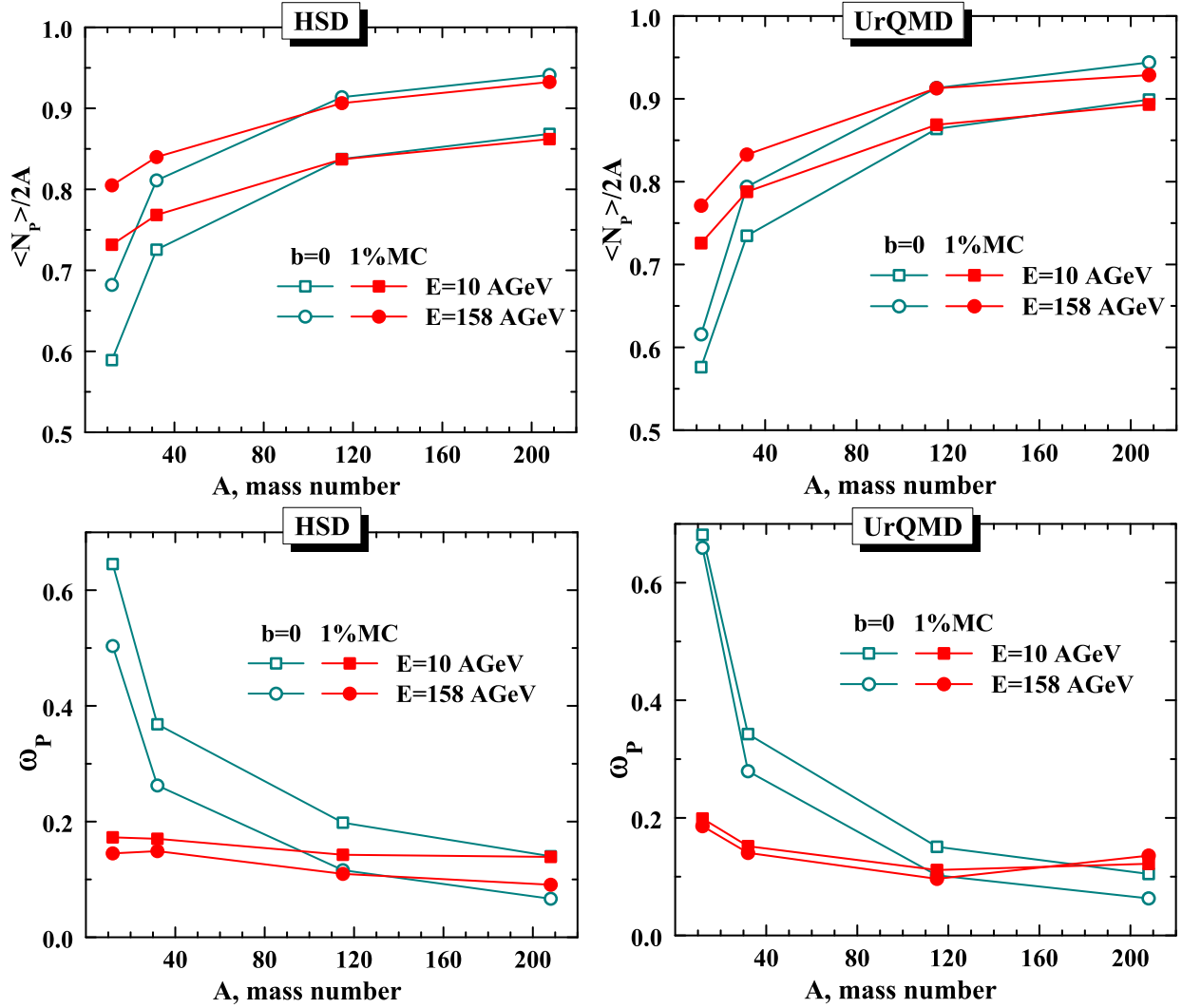


FIG. 7: (Color online) The HSD (*left*) and UrQMD (*right*) results for the ratio $\langle N_P \rangle / 2A$ (the upper panel) and the scaled variance of the participant number fluctuations, ω_P (the lower panel), for the 1% most central collisions selected by the largest values of N_P^{proj} (full symbols), for different nuclei at collision energies $E_{lab}=10$ and 158 AGeV. The open symbols present the results of Fig. 3 (*right*) for $b = 0$.

multiplicity N at a given value of b . This is valid if c is not too small and the colliding nuclei are not too light. In the sample of A+A events with 1% of largest N_P^{proj} , the relation (5) can not be applied for S+S and C+C collisions. The average value of $\langle N_P^{proj} \rangle$ even for $b = 0$ is essentially smaller than its maximal value A . To form the sample with 1% largest N_P^{proj} , one needs at several fixed values of b to take into account the *fluctuations* with $N_P^{proj} > \langle N_P^{proj}(b) \rangle$.

Just the fluctuations of the number of nucleon participants form the 1% sample with largest

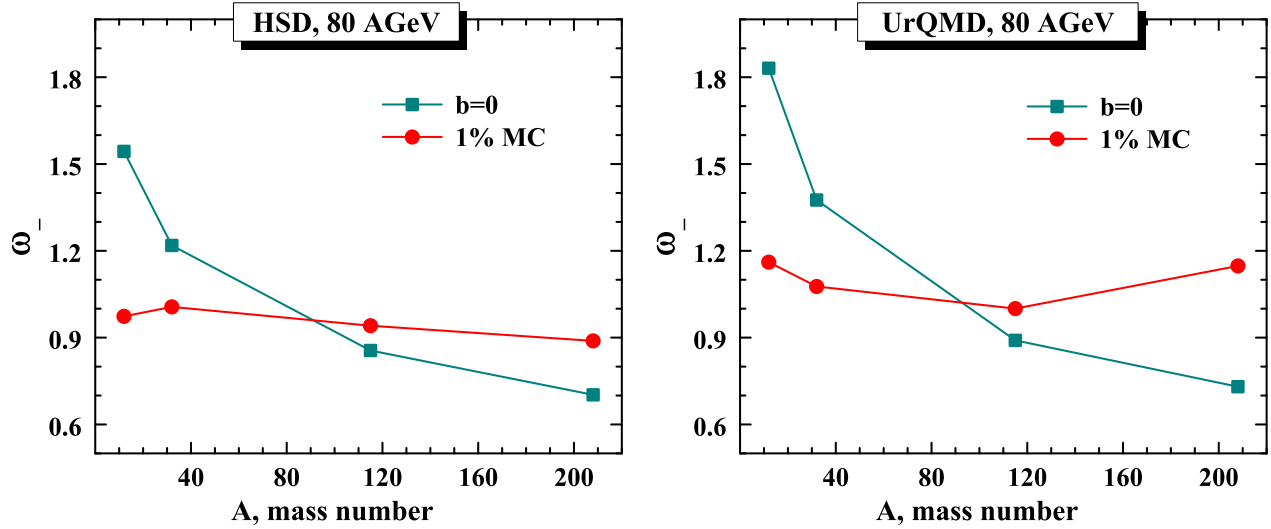


FIG. 8: (Color online) The dependence of ω_- on atomic mass number at $E_{lab}=80$ AGeV for the HSD (*left*) and UrQMD (*left*) simulations. The squares correspond to $b = 0$, and circles to 1% largest N_P^{proj} .

N_P^{proj} values.

Fig. 8 shows a comparison of the A -dependence of ω_- in the transport models for two different samples of the collision events: for $b = 0$ and for the 1% of events with largest N_P^{proj} values. One can see that the multiplicity fluctuations are rather different in these two samples. Moreover, these differences are in the opposite directions for heavy nuclei and for light nuclei. For light nuclei, ω_- is essentially smaller in the 1% sample with largest N_P^{proj} values, whereas for heavy nuclei the smaller fluctuations correspond to $b = 0$ events. Note that in the 1% sample with largest N_P^{proj} values the A -dependence of multiplicity fluctuations becomes much weaker. In this case, a strong increase of the multiplicity fluctuations for light nuclei, seen for $b = 0$, disappears.

For the 1% most central $A + A$ collision events - selected by the largest values of N_P^{proj} - the HSD multiplicity fluctuations are shown in Figs. 9 and 11 and the corresponding UrQMD results are shown in Figs. 10 and 12. The results from both models are also presented in Table I. The model uncertainties are shown as errorbars in Figs. 9 and 10. For light nuclei (S and C) the multiplicity fluctuations in the samples of 1% most central collisions are smaller than in the $b = 0$ selection and the atomic mass number dependencies become less pronounced (compare Figs. 9 and 10 with Fig. 4). This is because the participant number fluctuations ω_P have now essentially smaller A -dependence, as seen in Fig. 7.

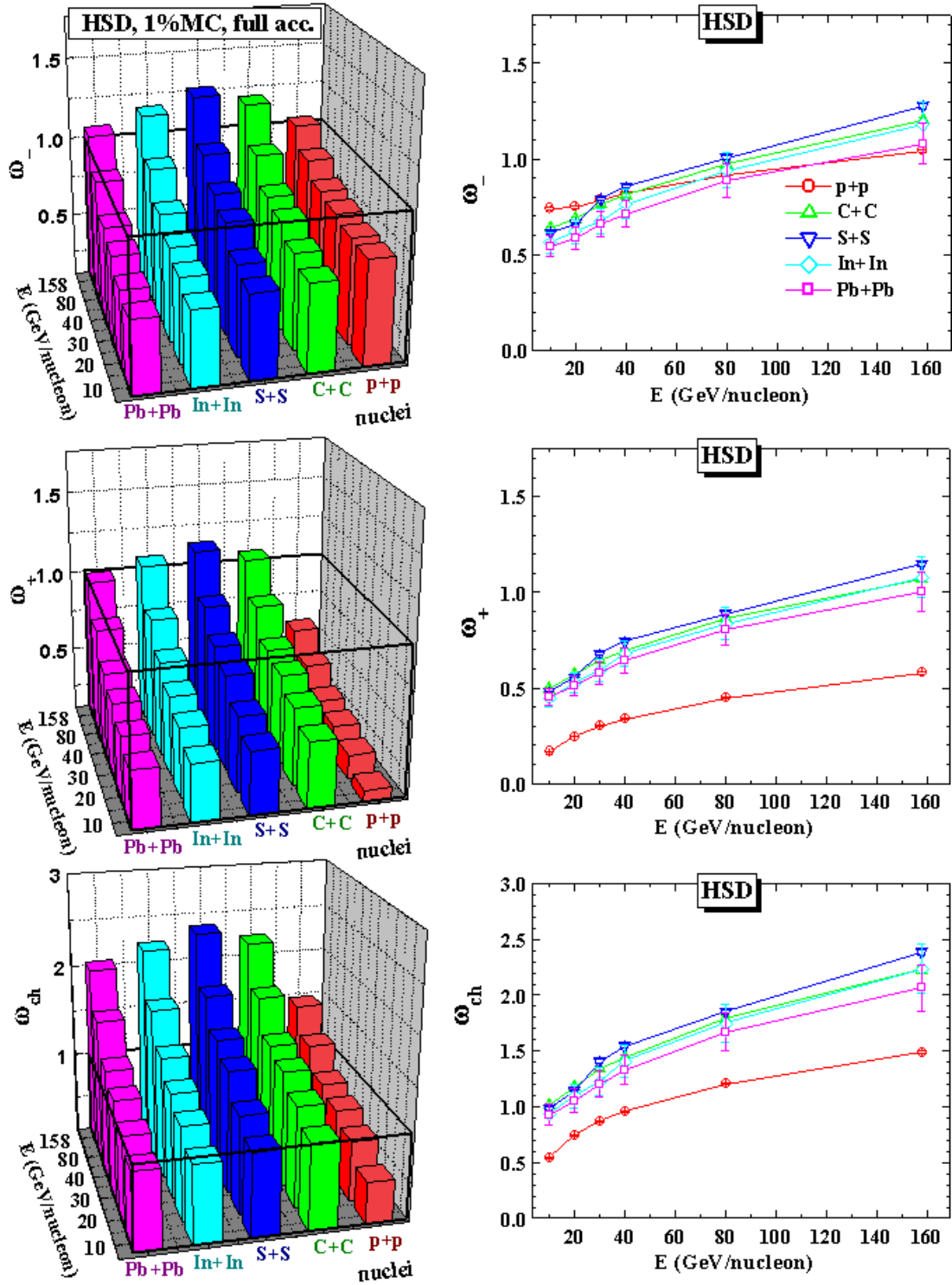


FIG. 9: (Color online) The HSD results for ω_- (upper panel), ω_+ (middle panel), and ω_{ch} (lower panel) in $A + A$ and $p+p$ collisions for the full 4π acceptance in 3D (*left*) and 2D (*right*) projection. The 1% most central C+C, S+S, In+In, and Pb+Pb collisions are selected by choosing the largest values of N_P^{proj} at different collision energies $E_{lab}=10, 20, 30, 40, 80, 158$ AGeV. The errorbars indicate the estimated uncertainties in the model calculations. The HSD results from inelastic $p+p$ collisions

		p+p			C+C			S+S			In+In			Pb+Pb		
		-	+	ch	-	+	ch	-	+	ch	-	+	ch	-	+	ch
HSD: full acc.	10	0.74	0.17	0.54	0.64	0.50	1.02	0.61	0.48	0.99	0.56	0.45	0.94	0.54	0.45	0.93
	20	0.75	0.25	0.74	0.69	0.57	1.18	0.66	0.55	1.14	0.62	0.53	1.10	0.58	0.51	1.05
	30	0.79	0.30	0.87	0.76	0.64	1.34	0.79	0.68	1.41	0.67	0.59	1.22	0.66	0.58	1.20
	40	0.82	0.34	0.96	0.81	0.69	1.44	0.86	0.75	1.54	0.76	0.68	1.41	0.71	0.64	1.33
	80	0.92	0.45	1.21	0.97	0.86	1.79	1.01	0.89	1.85	0.94	0.84	1.75	0.89	0.80	1.67
	158	1.04	0.58	1.49	1.20	1.07	2.23	1.28	1.15	2.39	1.18	1.08	2.24	1.08	1.00	2.07
HSD: $y > 0$	10	0.85	0.33	0.53	0.73	0.53	0.77	0.72	0.52	0.76	0.71	0.54	0.77	0.68	0.56	0.76
	20	0.83	0.39	0.68	0.73	0.56	0.86	0.70	0.56	0.83	0.68	0.56	0.82	0.69	0.59	0.82
	30	0.83	0.42	0.77	0.74	0.58	0.91	0.76	0.59	0.94	0.69	0.60	0.87	0.69	0.63	0.90
	40	0.84	0.44	0.82	0.74	0.62	0.97	0.80	0.62	1.01	0.74	0.63	0.98	0.75	0.64	0.98
	80	0.88	0.49	0.96	0.82	0.69	1.16	0.83	0.70	1.17	0.80	0.70	1.13	0.77	0.71	1.11
	158	0.94	0.58	1.16	0.94	0.78	1.39	0.96	0.79	1.41	0.93	0.80	1.38	0.93	0.80	1.34
UrQMD: full acc.	10	0.69	0.15	0.49	0.62	0.54	1.05	0.57	0.43	0.89	0.53	0.41	0.85	0.59	0.47	0.98
	20	0.82	0.25	0.77	0.71	0.63	1.25	0.65	0.55	1.12	0.59	0.49	1.02	0.72	0.64	1.30
	30	0.90	0.34	0.96	0.83	0.73	1.48	0.77	0.68	1.38	0.67	0.58	1.20	0.79	0.71	1.45
	40	0.97	0.41	1.13	0.93	0.84	1.70	0.87	0.76	1.57	0.77	0.68	1.40	0.87	0.79	1.61
	80	1.18	0.59	1.56	1.16	1.05	2.15	1.08	0.97	1.99	1.00	0.89	1.85	1.15	1.07	2.18
	158	1.33	0.76	1.93	1.47	1.34	2.76	1.38	1.24	2.57	1.33	1.22	2.51	1.70	1.61	3.27
UrQMD: $y > 0$	10	0.84	0.43	0.63	0.69	0.56	0.80	0.71	0.55	0.80	0.67	0.53	0.77	0.71	0.56	0.83
	20	0.89	0.48	0.82	0.74	0.63	0.96	0.73	0.60	0.90	0.74	0.56	0.87	0.76	0.65	0.99
	30	0.91	0.55	0.97	0.82	0.67	1.10	0.77	0.65	1.02	0.73	0.63	0.96	0.78	0.69	1.06
	40	0.98	0.62	1.09	0.83	0.74	1.20	0.83	0.70	1.14	0.77	0.67	1.05	0.81	0.72	1.13
	80	1.02	0.68	1.31	0.96	0.83	1.46	0.90	0.81	1.37	0.85	0.78	1.27	0.92	0.85	1.41
	158	1.19	0.69	1.46	1.08	0.96	1.74	1.07	0.95	1.70	1.02	0.95	1.66	1.18	1.12	1.96

TABLE I: The HSD and UrQMD scaled variances ω_- , ω_+ , and ω_{ch} for the 1% of most central collisions selected by largest values of N_P^{proj} . The numbers correspond to those presented in Figs. 9–12.

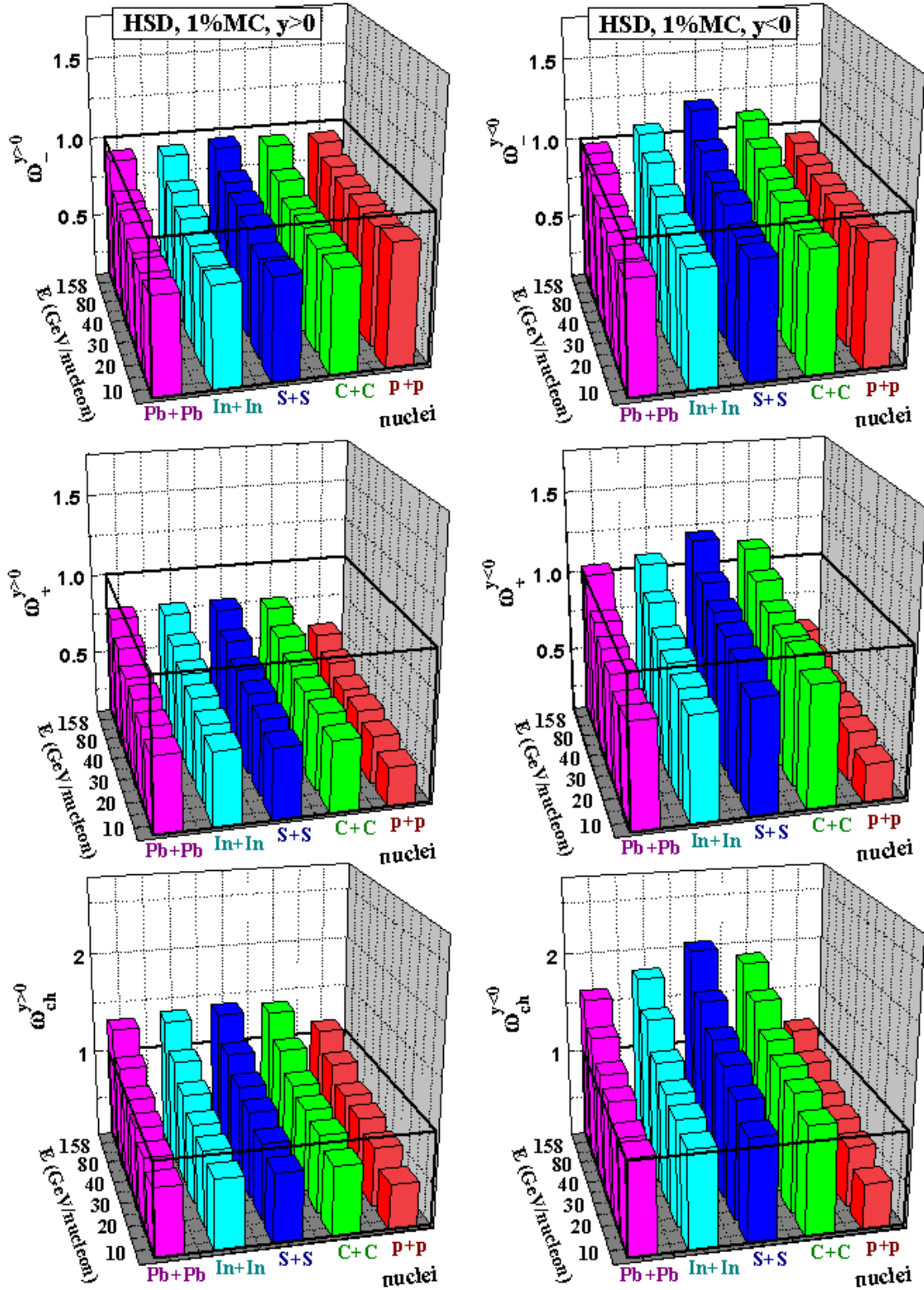


FIG. 11: (Color online) The same as in Fig. 9, but for final hadrons accepted in the projectile hemisphere, $y > 0$ (left), and in the target hemisphere, $y < 0$ (right). The HSD results in inelastic p+p collisions are the same as in Fig. 5.

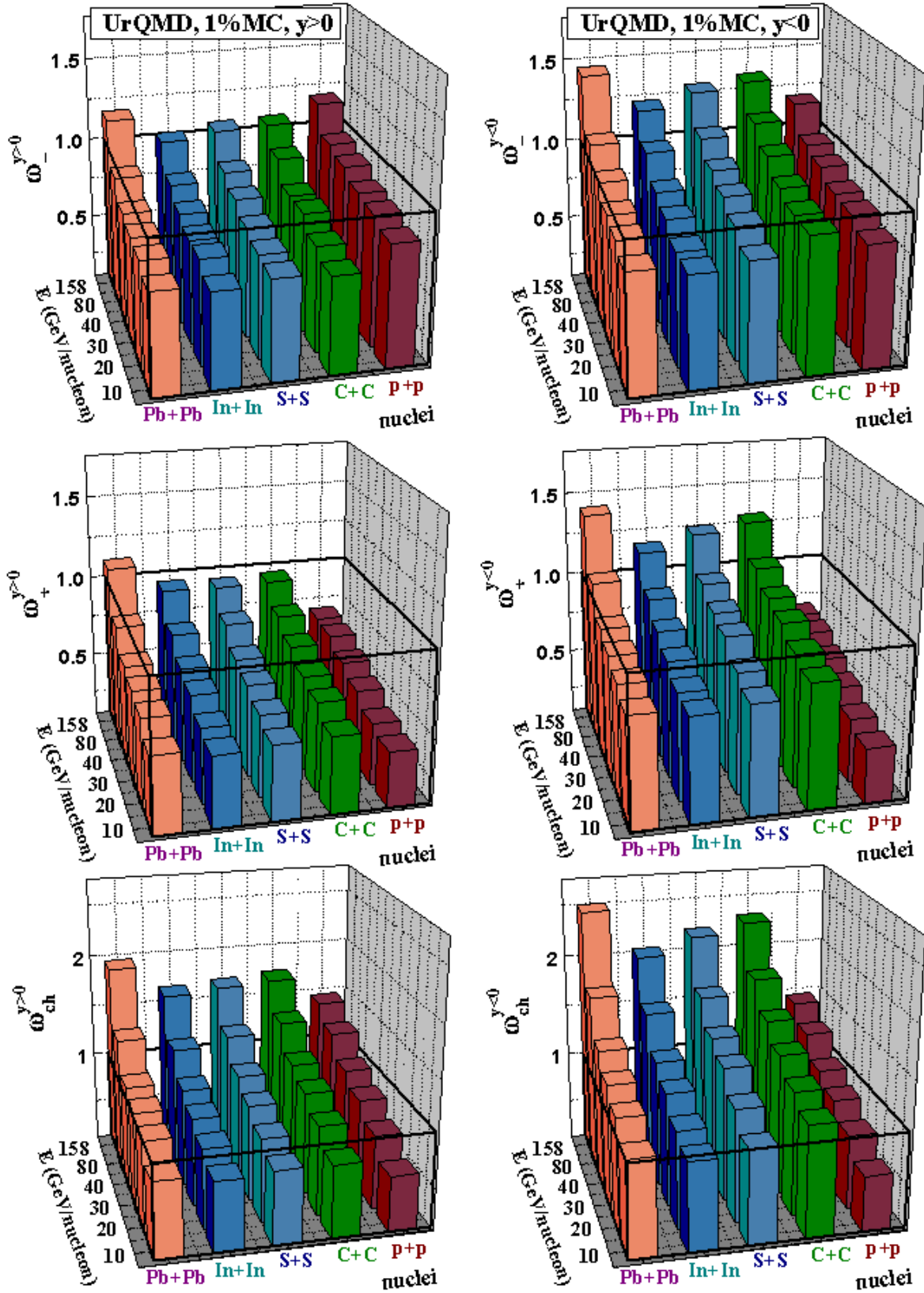


FIG. 12: (Color online) The same as in Fig. 11, but for the UrQMD.

Fig. 4 shows that both HSD and UrQMD predict a monotonic dependence of the charge particle multiplicity with energy. So, the hadronic ‘background’ for the NA61 experiments is expected to be a smooth monotonic function of beam energy.

Besides of differences in the realization of the string fragmentation model in HSD and UrQMD 1.3 mentioned above (cf. Fig. 1), additional deviations can be attributed to different initializations of the nuclei in both models. Indeed, the event-by-event observables show a higher sensitivity to the initial nucleon density distribution than the standard single particle observables [25]. A pilot study using UrQMD shows different ω when applying different initialization shapes. Due to this effects a systematic error of 20% is attributed to ω . Such a sensitivity of the A-dependence of ω_{ch} to the details of the models indicates a necessity for further studies of the initializations of the nuclei in transport model approaches. This becomes important for the theoretical interpretation of future experimental data on event-by-event fluctuations.

Note that the model of independent sources and Eq. (4) work for the multiplicity fluctuations simulated by the transport models in full 4π acceptance but not for the acceptance in a specific rapidity region. The results for inelastic p+p collisions are identical in the projectile and target hemispheres. This is not the case in the sample of 1% most central $A + A$ collisions selected by N_P^{proj} . The total number of nucleons participating in $A + A$ collisions fluctuates. These fluctuations are not symmetric in forward-backward hemispheres: in the selected 1% sample the number of target participants N_P^{targ} fluctuates essentially stronger than that of N_P^{proj} . The consequences of the asymmetry in an event selection depend on the dynamics of A+A collision (see Ref. [23] for details). The HSD and UrQMD results in Figs. 11 and 12 clearly demonstrate larger values for all scaled variances, ω_- , ω_+ , and ω_{ch} , for $y < 0$ acceptance than those for $y > 0$ one. This is due to stronger target participant fluctuations, $\omega_P^{targ} > \omega_P^{proj}$.

VI. SUMMARY AND CONCLUSIONS

In summary, the event-by-event multiplicity fluctuations in nucleus-nucleus collisions have been studied for different energies and system sizes within the HSD and UrQMD v. 1.3 transport approaches. Our present study is in full correspondence to the future experimental program of the NA61 Collaboration at the SPS. Thus we have considered C+C, S+S, In+In, and Pb+Pb nuclear collisions from $E_{lab} = 10, 20, 30, 40, 80, 158$ AGeV. The influence of participant number fluctuations on hadron multiplicity fluctuations has been emphasized and studied in

detail. To make these ‘trivial’ fluctuations smaller, one has to consider the most central collisions. Indeed, one needs to make a very rigid selection – 1% or smaller – of the ‘most central’ collision events. In addition, one wants to compare the event-by-event fluctuations in these ‘most central’ collisions for heavy and for light nuclei. Under these new requirements different centrality selections are not equivalent to each other. As a consequence, there is no universal geometrical selection by the impact parameter. This is a new and serious problem for theoretical models (e.g., for hydrodynamical models) in a precision description of the event-by-event fluctuation data. The above statements have been illustrated by the $b = 0$ selection criterium considered in our paper. For light nuclei even these ‘absolutely central’ geometrical collisions lead to rather large fluctuations of the number of participants, essentially larger than in the 1% most central collisions selected by the largest values of the projectile participants N_P^{proj} .

We have, furthermore, used the number of projectile participants to define the centrality selection. This is the most promising way of the centrality selection in fixed target experiments. It also corresponds to the experimental plans of the NA61 collaboration. We have defined the 1% most central collisions by selecting the largest values of the projectile participants N_P^{proj} . The multiplicity fluctuations calculated in these samples show a much weaker dependence on the atomic mass number A than for criterium $b = 0$. A monotonic energy dependence for the multiplicity fluctuations are obtained in both the HSD and UrQMD transport models. The two models demonstrate a similar qualitative behavior of the particle number fluctuations. However, the UrQMD 1.3 results for the scaled variances ω_- , ω_+ , and ω_{ch} are systematically larger than those obtained within HSD. This is mainly due to the corresponding inequalities for the scaled variances ω_{ch} (see Fig. 1, *right*) for p+p collisions in these models. Our study has demonstrated a sensitivity of the multiplicity fluctuations to some specific details of the transport models. Nevertheless, the present HSD and UrQMD results for the scaled variances provide a general trend of their dependencies on A and E_{lab} and also indicate quantitatively the systematic uncertainties.

We stress again, that HSD and UrQMD do not include explicitly a phase transition to the QGP. The expected enhanced fluctuations - attributed to the critical point and phase transition - can be observed experimentally on top of a monotonic and smooth ‘hadronic background’. The most promising signature of the QCD critical point would be an observation of a non-monotonic dependence of the scaled variances on bombarding energy E_{lab} for central A+A collisions with

fixed atomic mass number. In the fixed target SPS experiments the centrality selection in A+A collisions is defined by the number of the projectile participants. The measurements of ω_- , ω_+ , and ω_{ch} are then preferable in the forward hemispheres. In this case the remaining small fluctuations of the number of target participants in the 1% most central collisions become even less important, as they contribute mainly to the particle fluctuations in the backward hemisphere. Our findings should be helpful for the optimal choice of collision systems and collision energies for the experimental search of the QCD critical point.

Acknowledgments

We like to thank V.V. Begun, M. Bleicher, W. Cassing, M. Gaździcki, W. Greiner, M. Hauer, and I.N. Mishustin for useful discussions.

-
- [1] H. Heiselberg, Phys. Rep. **351**, 161 (2001).
- [2] S. Jeon and V. Koch, Review for Quark-Gluon Plasma 3, eds. R.C. Hwa and X.-N. Wang, World Scientific, Singapore, 430-490 (2004) [arXiv:hep-ph/0304012].
- [3] T.K. Nayak, arXiv:0706.2708 [nucl-ex].
- [4] M. Gazdzicki, M. I. Gorenstein, and S. Mrowczynski, Phys. Lett. B **585**, 115 (2004); M. I. Gorenstein, M. Gazdzicki, and O. S. Zozulya, *ibid.* **585**, 237 (2004).
- [5] I.N. Mishustin, Phys. Rev. Lett. **82**, 4779 (1999); Nucl. Phys. A **681**, 56c (2001); H. Heiselberg and A.D. Jackson, Phys. Rev. C **63**, 064904 (2001).
- [6] M.A. Stephanov, K. Rajagopal, and E.V. Shuryak, Phys. Rev. Lett. **81**, 4816 (1998); Phys. Rev. D **60**, 114028 (1999); M.A. Stephanov, Acta Phys. Polon. B **35**, 2939 (2004);
- [7] S.V. Afanasev *et al.*, [NA49 Collaboration], Phys. Rev. Lett. **86**, 1965 (2001); M.M. Aggarwal *et al.*, [WA98 Collaboration], Phys. Rev. C **65**, 054912 (2002); J. Adams *et al.*, [STAR Collaboration], *ibid.* **68**, 044905 (2003); C. Roland *et al.*, [NA49 Collaboration], J. Phys. G **30** S1381 (2004); Z.W. Chai *et al.*, [PHOBOS Collaboration], J. Phys. Conf. Ser. **37**, 128 (2005); M. Rybczynski *et al.* [NA49 Collaboration], J. Phys. Conf. Ser. **5**, 74 (2005); C. Alt *et al.*, [NA49 Collaboration], Phys. Rev. C **75** (2007) 064904.
- [8] H. Appelshauser *et al.* [NA49 Collaboration], Phys. Lett. B **459**, 679 (1999); D. Adamova *et al.*, [CERES Collaboration], Nucl. Phys. A **727**, 97 (2003); T. Anticic *et al.*, [NA49 Collaboration], Phys. Rev. C **70**, 034902 (2004); S.S. Adler *et al.*, [PHENIX Collaboration], Phys. Rev. Lett. **93**, 092301 (2004); J. Adams *et al.*, [STAR Collaboration], Phys. Rev. C **71**, 064906 (2005).
- [9] V.V. Begun *et al.*, Phys. Rev. C **70**, 034901 (2004); *ibid.* **71**, 054904 (2005); *ibid.* **74**, 044903 (2006); M. Hauer, V.V. Begun, and M.I. Gorenstein, arXiv:0706.3290 [nucl-th]; M. Hauer, arXiv:0710.3938 [nucl-th].
- [10] V.P. Konchakovski, *et al.*, Phys. Rev. C **73**, 034902 (2006);
- [11] V.P. Konchakovski, *et al.*, Phys. Rev. C **74**, 064911 (2006).
- [12] F. Becattini, J. Manninen, and M. Gazdzicki, Phys. Rev. C **73** (2006) 044905.
- [13] V.V. Begun, M. Ga'zdicki, M.I. Gorenstein, M. Hauer, V.P. Konchakovski, and B. Lungwitz, Phys. Rev. C **76**, 024902 (2007).
- [14] V.P. Konchakovski, M.I. Gorenstein, and E.L. Bratkovskaya, Phys. Lett. **B651**, 114 (2007).

- [15] B. Lungwitz and M. Bleicher, Phys. Rev. **C76**, 044904 (2007).
- [16] B. Lungwitz *et al.* [NA49 Collaboration], arXiv:nucl-ex/0610046; C. Alt *et al.*, arXiv:0712.3216.
- [17] S.S. Adled *et al.* [PHENIX Collaboration], Phys. Rev. C **71**, 034908 (2005); *ibid.* **71**, 049901 (2005); J. Mitchell [PHENIX Collaboration], J. Phys. Conf. Ser. **27**, 88 (2005).
- [18] V.P. Konchakovski, M.I. Gorenstein, and E.L. Bratkovskaya, Phys. Rev. C **76**, 031901(R) (2007).
- [19] M. Gazdzicki *et al.* [NA61 Collaboration], PoS C **POD2006**, 016 (2006) [arXiv:nucl-ex/0612007]; N. Antoniou *et al.* [NA61 Collaboration], “Study of hadron production in hadron nucleus and nucleus nucleus collisions at the CERN SPS,” CERN-SPSC-P-330 (2006).
- [20] W. Ehehalt and W. Cassing, Nucl. Phys. A **602**, 449 (1996); W. Cassing and E.L. Bratkovskaya, Phys. Rep. **308**, 65 (1999).
- [21] S.A. Bass *et al.*, Prog. Part. Nucl. Phys. **41**, 255 (1998); M. Bleicher *et al.*, J. Phys. G **25**, 1859 (1999).
- [22] H. Weber, *et al.*, Phys. Rev. **C67**, 014904 (2003); E.L. Bratkovskaya, *et al.*, *ibid.* **67**, 054905 (2003); *ibid.*, **69**, 054907 (2004); Prog. Part. Nucl. Phys. **53**, 225 (2004); Phys. Rev. Lett., **92**, 032302 (2004).
- [23] M. Gaździcki and M. Gorenstein, Phys. Lett. **B640**, 155 (2006).
- [24] W. Broniowski and W. Florkowski, Phys. Rev. C **65**, 024905 (2002).
- [25] B. Mattos Tavares, H.-J. Drescher, and T. Kodama, arXiv:hep-ph/0702224.